

BCS-BEC crossover in bilayers of cold fermionic polar moleculesN. T. Zinner,^{1,2,3} B. Wunsch,¹ D. Pekker,^{1,4} and D.-W. Wang^{5,6,7}¹*Department of Physics, Harvard University, Cambridge, Massachusetts 02138, USA*²*Department of Physics and Astronomy, Aarhus University, Aarhus C, DK-8000, Denmark*³*The Niels Bohr Institute, University of Copenhagen, Copenhagen Ø, DK-8000, Denmark*⁴*Department of Physics, California Institute of Technology, Pasadena, California 91125, USA*⁵*Physics Department, National Tsing-Hua University, Hsinchu 300, Taiwan*⁶*Physics Division, National Center for Theoretical Sciences, Hsinchu 300, Taiwan*⁷*Frontier Research Center on Fundamental and Applied Sciences of Matters, National Tsing-Hua University, Hsinchu 300, Taiwan*

(Received 10 September 2010; revised manuscript received 10 February 2011; published 3 January 2012)

We investigate the quantum and thermal phase diagram of fermionic polar molecules loaded in a bilayer trapping potential with perpendicular dipole moment. We use both a BCS-theory approach that is most reliable at weak coupling and a strong-coupling approach that considers the two-body bound dimer states with one molecule in each layer as the relevant degree of freedom. The system ground state is a Bose-Einstein condensate (BEC) of dimer bound states in the low-density limit and a paired superfluid (BCS) state in the high-density limit. At zero temperature, the intralayer repulsion is found to broaden the regime of BCS-BEC crossover and can potentially induce system collapse through the softening of roton excitations. The BCS theory and the strongly coupled dimer picture yield similar predictions for the parameters of the crossover regime. The Berezinskii-Kosterlitz-Thouless transition temperature of the dimer superfluid is also calculated. The crossover can be driven by many-body effects and is strongly affected by the intralayer interaction which was ignored in previous studies.

DOI: [10.1103/PhysRevA.85.013603](https://doi.org/10.1103/PhysRevA.85.013603)

PACS number(s): 67.85.-d, 03.75.Ss, 74.78.-w

I. INTRODUCTION

Recent progress in trapping and cooling of polar molecules [1–6] has enabled studies of many-body systems with long-range anisotropic dipole-dipole forces, where new exotic phases might exist [7,8]. The attractive part of the interaction can, however, lead to chemical reaction losses [6]. A way to stabilize the system is to load molecules in a one- or two-dimensional optical lattice, where interesting low-dimensional physics has been predicted [9–17]. A prominent example is polar fermions loaded in a bilayer system with dipoles oriented perpendicular to the layer plane [18]. In the limit of high density or weak interaction, the system is very similar to conventional superconductors, and the ground state should be a BCS state [with interactions as in Fig. 1(a)]. In the dilute limit, it is known that the interlayer interaction always supports a bound state [19–21], and the ground state should be a Bose-Einstein condensate (BEC) of dimers [Fig. 1(b)]. As a result, the BCS-BEC crossover in this bilayer system could be richer than in the usual atomic Fermi gas, where crossover is driven by the two-body physics of a Feshbach resonance [22]. Here it is driven by many-body effects which depend not only on the interaction strength but also on the density. Furthermore, the intralayer repulsion can cause roton softening and/or Wigner crystallization in the high-density limit [15–17]. Therefore, a many-body theory including both intra- and interlayer interactions is not only of quantitative interest but also qualitatively important.

In this paper, we study the quantum and thermal phase diagrams of fermionic polar molecules loaded in a bilayer system including both *intra-* and *interlayer* interaction. The quantum phase diagram is shown in Fig. 1(c). BCS (BEC) ground states are found in the limit of weak (strong) interaction and large (small) density. In between, we have the crossover regime (crossover I), which can be determined by the chemical

potential calculated from many-body theories in the different limits (see below). When intralayer repulsion is neglected, the crossover region (crossover II) moves to lower interaction strength. In addition, intralayer interactions could perhaps give rise to a roton instability at large density and strong interaction, although further analysis beyond the scope of this work is needed. We also determine the Berezinskii-Kosterlitz-Thouless (BKT) critical temperature [23,24] in the strongly coupled regime, including the effective interaction of the dimers. The maximum critical temperature obtained is one-tenth of the Fermi energy and should therefore be achievable in experimental setups in the near future.

We note that two other recent studies have considered a system similar to the one studied here. The paper by Pikovski *et al.* [25] considers the BCS and BEC phases based on BCS theory at both zero and finite temperature. However, these authors do not consider the full effect of the intralayer interaction. When we neglect the intralayer interaction, our results are consistent with those of Ref. [25]. A related study by Baranov *et al.* [26] addresses the critical temperature for the superfluid phase in the weak-coupling limit, taking particle-hole correlations also into account. In contrast, here we consider the finite-temperature phase diagram from the strong-coupling limit. Extrapolation of our results to the parameter regime of Ref. [26] would exceed the boundaries of our approximations, and the current study should be viewed as complementary to Ref. [26].

Our model and the assumptions we use are described Sec. II. In Sec. III, we discuss the case of zero temperature and the role of intralayer interactions in the BCS-BEC crossover. This is achieved by considering the physics from both a weak- and a strong-coupling point of view. The two approaches are shown to yield consistent results. We proceed to discuss the finite-temperature phase diagram in Sec. IV. Here we calculate the

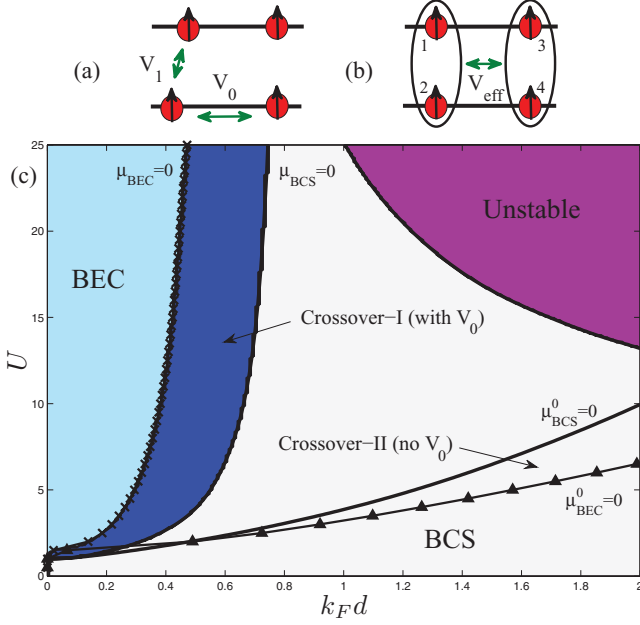


FIG. 1. (Color online) Schematic of a few particles in a bilayer with (a) inter- (V_1) and intralayer (V_0) interactions in the BCS limit and (b) the effective interaction (V_{eff}) between the dimers in the BEC limit (see text). (c) Quantum phase diagram for a bilayer with fermionic polar molecules in the interaction-density plane. Interactions are characterized by $U = mD^2/\hbar^2d$ and by k_Fd , where m , D , d , and k_F are respectively the molecular mass, dipole moment, interlayer distance, and Fermi momentum. The crossover I region includes the effect of intralayer interactions, while the crossover II region does not. In the upper right-hand corner we speculate that the system could potentially display a roton instability as discussed in the text.

critical temperature for the superfluid phase within mean-field theory and using the universal relation for the BKT transition temperature. Section V contains a summary, a discussion of experimental parameters to realize the predicted phases and an outlook for future work.

II. MODEL

The Hamiltonian for polar molecules in the bilayer system is given by $H = \sum_{k\sigma} \epsilon_k c_{k,\sigma}^\dagger c_{k,\sigma} + \frac{1}{2\Omega} \sum_{\mathbf{q}\mathbf{k}\mathbf{k}',\sigma\sigma'} V_{\sigma\sigma'}(\mathbf{q}) c_{\mathbf{k}+\mathbf{q},\sigma}^\dagger c_{\mathbf{k}'-\mathbf{q},\sigma'}^\dagger c_{\mathbf{k}',\sigma'} c_{\mathbf{k},\sigma}$, where Ω is the area of the layer plane, $\epsilon_k = \hbar^2 k^2/2m$, and $\sigma = \pm$ is the layer index. $V_{+-} = V_{-+} = V_1$ denotes the interlayer interaction and $V_{++} = V_{--} = V_0$ is the intralayer one. Here we neglect interlayer tunneling. We assume occupation of only the ground state in the transverse direction so that the transverse degree of freedom is a simple Gaussian that can be integrated out. This yields $V_0(\mathbf{q}) = \frac{8\pi D^2}{3\sqrt{2\pi}W} [1 - \frac{3}{2}F(|\mathbf{q}|)]$ and $V_1(\mathbf{q}) \rightarrow -2\pi D^2 |\mathbf{q}| e^{-|\mathbf{q}|d}$ as $W/d \rightarrow 0$. Here \mathbf{q} is the in-plane momentum, D is the dipole moment, W and d the layer width and interlayer spacing, and $F(q) = \sqrt{\pi/2} Wq [1 - \text{Erf}(Wq/\sqrt{2})] e^{q^2 W^2/2}$ with $\text{Erf}(x)$ the error function. The interlayer interaction is exact in the strict two-dimensional (2D) limit ($W \ll d$), but we find it is accurate enough ($<10\%$) at $W = 0.2d$, which is the value

used throughout. In the weak-interaction limit, the intralayer repulsion should renormalize the single-particle dispersion as in Fermi-liquid theory. If the layer index is treated as a spin degree of freedom, the gap equation is

$$\Delta_k = -\frac{1}{\Omega} \sum_{\mathbf{q}} \frac{V_1(\mathbf{k}-\mathbf{q})\Delta_{\mathbf{q}}}{2E_{\mathbf{q}}} \tanh\left(\frac{E_{\mathbf{q}}}{2k_B T}\right), \quad (1)$$

where $E_{\mathbf{q}} = \sqrt{\xi_{\mathbf{q}}^2 + |\Delta_{\mathbf{q}}|^2}$ is the quasiparticle dispersion, and $\xi_{\mathbf{q}} \equiv \epsilon_{\mathbf{q}} + \Sigma(\mathbf{q}) - \mu_{\text{BCS}}$. The self-energy $\Sigma(\mathbf{q})$ in the Hartree-Fock approximation is [27] $\Sigma(\mathbf{k}) = \frac{1}{2\Omega} \sum_{\mathbf{q}} [V_0(0) - V_0(\mathbf{k}-\mathbf{q})][1 - \frac{\xi_{\mathbf{q}}}{E_{\mathbf{q}}} \tanh(E_{\mathbf{q}}/2k_B T)]$. To access the crossover regime, the chemical potential μ_{BCS} must be determined self-consistently via the density equation

$$n = \frac{1}{2\Omega} \sum_{\mathbf{q}} \left[1 - \frac{\xi_{\mathbf{q}}}{E_{\mathbf{q}}} \tanh\left(\frac{E_{\mathbf{q}}}{2k_B T}\right) \right]. \quad (2)$$

We use the first Born approximation (FBA) with a realistic finite layer width for both intra- and interlayer interactions in Eq. (1). The exponentially decreasing shape of $V_1(\mathbf{q})$ means that use of the renormalized gap equations or the FBA yields similar results as noted already in Ref. [25]. The FBA is generally poor at strong coupling. However, since the crossover takes place at low density, we treat the intralayer in a weak-coupling sense in the current work. Inclusion of higher-order terms will be considered in future work.

Since the interlayer interaction V_1 is attractive at short distance, the dominant gap is s wave. Therefore, for simplicity, we neglect higher-partial-wave components and calculate $\Delta_k = \Delta_{|k|}$ from Eq. (1) by iteration. In Fig. 2(a), we show Δ_k/Δ_0 for different values of the dimensionless coupling $U = mD^2/\hbar^2d$ with $k_Fd = \sqrt{4\pi n}d^2 = 0.4$. When U is small, the maximum of $\Delta(k)$ is at $k/k_F = 2.5$, which is where $V_1(k)$

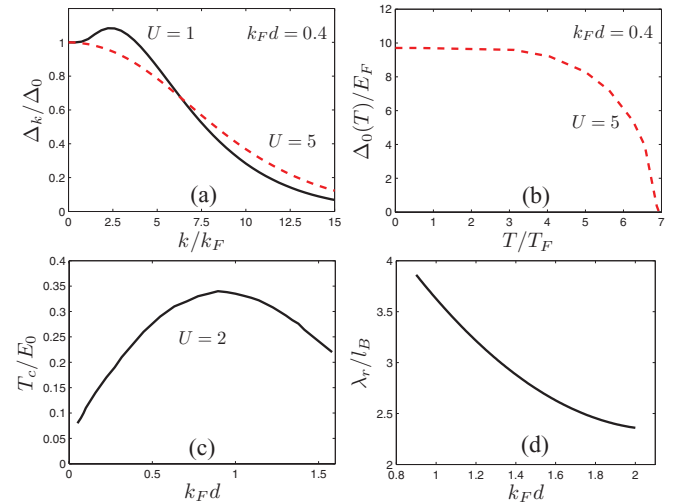


FIG. 2. (Color online) (a) Normalized gap Δ_k/Δ_0 as a function of k/k_F at $k_Fd = 0.4$ and $U = 1$ (solid) and $U = 5$ (dashed). (b) Temperature dependence of $\Delta_0(T)/E_F$ as a function of T/T_F for $k_Fd = 0.4$ ($E_F = 0.16E_0$). (c) BCS critical temperature as a function of k_Fd at $U = 2$ in units of $E_0 = \hbar^2/2md^2$. (d) Ratio of the roton wavelength λ_r at the instability to the dimer size l_B as a function of k_Fd .

is most attractive. When U is larger, the intralayer interaction renormalizes the single-particle dispersion; the structure of Δ_k disappears and the maximum is at $k = 0$. In Fig. 2(b) we show $\Delta_0(T)/E_F$ as a function of T/T_F , where E_F and T_F are the Fermi energy and temperature.

III. ZERO-TEMPERATURE RESULTS: INTRALAYER-INTERACTION EFFECTS ON THE BCS-BEC CROSSOVER

When the density is reduced, the ground state is expected to be a dimer BEC. Within BCS theory, this regime can be defined by having a negative chemical potential ($\mu_{\text{BCS}} < 0$). From Eq. (2), we can determine the $\mu_{\text{BCS}} = 0$ boundary as shown in Fig. 1(c). The two solid lines that bound the two crossover regions are calculated by including (μ_{BCS}) and neglecting (μ_{BCS}^0) the intralayer repulsion respectively. As expected, the repulsion strongly suppresses the $\mu_{\text{BCS}} < 0$ region, and for densities larger than a critical value of $k_F d \sim 0.77$, μ_{BCS} is positive for any U . We always find a $\mu_{\text{BCS}}^0 < 0$ region when the intralayer interaction is neglected. This shows that the intralayer interaction brings not only quantitative contributions but also qualitative and important changes of the quantum phase diagram. The effect of intralayer repulsion on the crossover physics can also be seen in the transition temperature T_c as shown in Fig. 2(c). It has a maximum at $k_F d \sim 1$, similar to crossover in a quasi-2D superconductor [28]. In contrast to BCS results for Fermi gases with short-range interaction, the decrease of T_c at high density is caused by the long-range intralayer repulsion.

In order to investigate the many-body physics of the BEC limit (i.e., the strong-interaction or low-density limit) in more detail, we go beyond BCS theory, which is based on Fermi-liquid theory at high density. Starting from the extremely dilute limit, the bound dimer is the main constituent with binding energy E_B . For small density, we neglect the intralayer term but include the Fermi pressure in the chemical potential: $\mu_{\text{BEC}}^0 = E_F - E_B/2$, where E_B is obtained numerically [19–21]. We define the crossover regime (crossover II) as the region bounded by $\mu_{\text{BCS}} = 0$ and $\mu_{\text{BEC}}^0 = 0$, the latter given by the line with triangles in Fig. 1(c). The crossover II region is quite narrow, which indicates that the BCS theory and the strong-coupling results are very similar. The expression for μ_{BCS}^0 given above holds exactly for zero-range interactions [29] and indicates that the crossover happens when the dimer size becomes comparable to the interparticle distance. While the interlayer dipole interaction behaves similar to a zero-range interaction, the intralayer dimer-dimer interaction can have significant effects on μ_{BEC} as we now demonstrate by deriving an effective interaction between dimers. We note that a recent Monte Carlo study of the BCS-BEC crossover in two dimensions also finds that, in the BEC limit, the dimer-dimer and atom-dimer interactions are important corrections that are not taken into account in the usual BCS theory without self-energy corrections [30].

The coordinates of the four molecules are denoted by $\mathbf{r}_1, \dots, \mathbf{r}_4$ as shown in Fig. 1(b), where $(\mathbf{r}_1, \mathbf{r}_2)$ are for the left dimer and $(\mathbf{r}_3, \mathbf{r}_4)$ for the right dimer. We are interested in a deep bound state, where the dimer size is smaller than the interdimer distance, i.e., $|\rho| \gg |\mathbf{r}|, |\mathbf{r}'|$, where $\rho = (\mathbf{r}_1 +$

$\mathbf{r}_2)/2 - (\mathbf{r}_3 + \mathbf{r}_4)/2$ is the interdimer distance and $\mathbf{r} = \mathbf{r}_1 - \mathbf{r}_2$ and $\mathbf{r}' = \mathbf{r}_3 - \mathbf{r}_4$ are the relative coordinates in each dimer. Straightforward algebra and integration over the dimer bound-state wave function $\phi(\mathbf{r})$ yield the effective dimer-dimer interaction $V_{\text{eff}}(\rho) = \int d\mathbf{r} d\mathbf{r}' |\phi(\mathbf{r})|^2 |\phi(\mathbf{r}')|^2 \sum_{s=\pm 1, \alpha=0,1} V_\alpha(\rho + s\mathbf{r}_\alpha)$, where $\mathbf{r}_{0,1} \equiv (\mathbf{r} \mp \mathbf{r}')/2$. In the strong-interaction and dilute-density limit, we can approximate $\phi(\mathbf{r})$ by a Gaussian profile: $\phi(\mathbf{r}) = (l_B \sqrt{\pi})^{-1} \exp(-|\mathbf{r}|^2/2l_B^2)$, where $l_B = \sqrt{2\hbar^2/mE_B}$ is the radius of the dimer bound state. As a result, V_{eff} has the following simple Fourier transform:

$$V_{\text{eff}}(\mathbf{k}) = [2V_1(\mathbf{k}) + 2V_0(\mathbf{k})] \exp(-|\mathbf{k}|^2 l_B^2/8). \quad (3)$$

The Gaussian approximation for $\phi(\mathbf{r})$ fails for $U \lesssim 2$; however, we have checked that our results are qualitatively unchanged if the exact solution is used [31]. Notice that V_{eff} takes the strong interlayer interaction into account through the dimer wave function. The FBA is used for the intralayer term, which is reasonable since the crossover happens at low density. For the roton instability, the FBA was used in quasi-2D studies of dipolar bosons [32,33], and we expect it to remain a fair approximation at larger densities as well. We note that dipolar interactions are different from short- or zero-range interactions. Zero-range interactions in 2D always allow a two-body dimer bound state [29], and a state of four bosons will also be bound [34]. This result is different from that in 3D, where the interaction must be sufficiently attractive to produce bound states. In the current setup, the dimer-dimer system is unbound [35].

The effective interaction has the property that $V_{\text{eff}}(0)$ is nonzero due to the intralayer term. However, the molecules are fermionic, and the Fock exchange contribution could cancel this term as is the case with true short-range interactions in interacting single-component Fermi gases. However, $V_{\text{eff}}(\mathbf{q})$ also has large contributions from $\mathbf{q}d > 0$, and this should have an influence on the phase diagram. This is supported by recent studies of the density-wave instability where the effect of exchange is found to be very large, shifting the instability into the strong-coupling regime [36–40]. The importance of exchange effects has also been discussed in relation to ferroelectricity with polar molecules [41]. Here we estimate the effects in the bosonic dimer limit by including the intralayer potential through $V_{\text{eff}}(0)$.

Using V_{eff} , the chemical potential in the BEC limit can be estimated as $\mu_{\text{BEC}} = nV_{\text{eff}}(0)/2 - E_B/2$ (we neglect the Fermi pressure, which is much smaller than the interaction energy for strong interactions). In Fig. 1(c), the solid line with crosses is given by $\mu_{\text{BEC}} = 0$ and is the upper bound of the crossover regime including intralayer interaction (crossover I). Notice in particular that the BEC region shrinks to lower density when the intralayer interaction is included, and there is no dimer condensate for $k_F d \gtrsim 0.42$. The ratio of interparticle distance to dimer size is 5 or more along the $\mu_{\text{BCS}} = 0$ and $\mu_{\text{BEC}} = 0$ lines. Without intralayer interaction the ratio is around 2.5, again demonstrating how the crossover physics is strongly modified by the intralayer term. We have estimate the chemical potential from both BCS and BEC limits, giving the bounds of the crossover regime with and without the intralayer interaction. Our results indicate that, in a realistic experiment,

the intralayer repulsion can significantly affect the regime where a dimer condensate is observable.

From the effective interaction between dimers, V_{eff} , we can also calculate the dispersion $\hbar\omega_d(\mathbf{k}) = \sqrt{\epsilon_k/2[\epsilon_k/2 + 2nV_{\text{eff}}(\mathbf{k})]}$ of the collective Bogoliubov mode of a dimer superfluid, in analogy to the case of dipolar bosons [33]. With increasing U we find roton softening around $kd = 2\pi$, which corresponds to a wavelength of $\lambda_r = 2\pi/k \sim d$. This softening leads to system collapse in the high-density and strong-interaction regime, as shown in Fig. 1(c). To investigate the nature of the instability, we plot λ_r/l_B in Fig. 2(d) and observe that λ_r is more than a factor of 2 larger than l_B for all densities. This implies that, at least in the low-density limit, it is a many-body effect.

The roton analysis assumes a well-defined dimer picture. We find the instability in the upper right-hand corner of Fig. 1(c), i.e., at higher densities and large U . While the dimer picture should prevail for large U , the higher densities imply that some fermionic nature could perhaps arise. A similar effect should arise in a fermionic picture but it is not easily calculated since fluctuations beyond BCS theory are needed. So at this point the findings for the roton instability remain speculative. This is an interesting topic for future work. We note that density waves in a single layer with fermionic polar molecules have been predicted recently [42,43]. A rough estimate indicates that the roton instability lies inside the region where a density wave in single layers is predicted. However, the authors of Refs. [42,43] neglect the Fock contributions, which are expected to be large [36–40]. The exact region of the density-wave instability is therefore not yet known. In any case, we expect the system to be unstable in the upper right part of the zero-temperature phase diagram of Fig. 1.

IV. FINITE-TEMPERATURE RESULTS: INTRALAYER-INTERACTION EFFECTS ON THE CRITICAL TEMPERATURE

We now investigate the finite-temperature phase diagram. In the BCS limit, we can use Eq. (1) to obtain the transition temperature T_c as shown by the dashed line in Fig. 3. We note that the intralayer interaction has very little influence on T_c at $k_F d = 0.4$. It is known that, in the weak-interaction limit, T_c is very close to the true transition temperature in a full BKT theory [44]. However, this calculation fails in the strong-interaction or dilute limit. At strong coupling, we obtain the BKT transition temperature from the universal relation $k_B T_{\text{BKT}} = \hbar^2 \pi n_s(T_{\text{BKT}})/2m$, where $n_s(T)$ is the superfluid density at temperature T [23,24]. According to Landau's two-fluid model, we have $n_s(T) = n - n_n(T)$, with normal-fluid density given by $n_n(T) = \frac{\hbar^2}{16mk_B T} \int \frac{d^2q}{(2\pi)^2} \left[\frac{q}{\sinh[\omega_d(q)/2k_B T]} \right]^2$ [45]. In Fig. 3 we show T_{BKT} of a dimer superfluid as a function of U for $k_F d = 0.4$ (solid black line). The dimer result differs from the BCS theory prediction in the weak-coupling limit, while it becomes saturated at $T_{\text{BKT}} = 0.125T_F$ for large U . In Ref. [25], T_c and T_{BKT} was calculated from the BCS superfluid state. For small U we find the same result for T_c . For dipolar bosons, the authors of Ref. [46] find $T_{\text{BKT}} \sim 0.1T_F$ for all values of U shown in Fig. 3. In order to compare to that study we need to

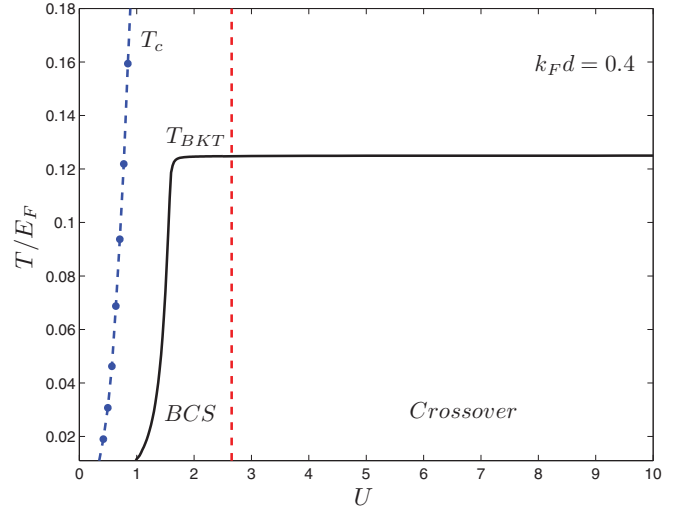


FIG. 3. (Color online) Transition temperature (T_{BKT} , solid black line) as a function of interaction strength for $k_F d = 0.4$. BCS result (T_c , dashed blue line) is shown for comparison. The dashed vertical line marks the position of $\mu_{\text{BCS}} = 0$ [see Fig. 1(c)].

assume point dimers with twice the dipole moment, which is of course not the case for small U , where T_{BKT} is reduced as the dimer size grows. Our strong-coupling dimer approach to the finite-temperature physics can be considered complementary to both Refs. [25,46]. The good agreement at intermediate and large U with the other approaches provides support that we capture the essential physics using the effective interaction between dimers.

V. DISCUSSION

We have studied fermionic polar molecules in a bilayer with perpendicularly polarized dipole moments. As the density and dipole strength vary, an analog (but with different physics) of the celebrated BCS-BEC crossover is predicted. We find that the intralayer repulsion (and dimer-dimer interaction) is crucial quantitatively and also to some extent qualitatively: It shrinks the region of dimer condensation so that no dimer state is expected when the density is larger than a critical value, and it also causes a roton instability in the high-density and strong-interaction regime. Our work is thus important for the study of BCS-BEC crossover physics in 2D systems, and our results should be observable within the parameter regime of near-future experiments.

It is worth stressing that our study considers the physics of the bilayer with fermionic polar molecules from different points of view. The BCS theory is usually more reliable in the weak-coupling regime, but can be extended into the crossover regime by solving the gap and number equations self-consistently. As the bilayer setup will always have a two-body bound state with one molecule in each layer, it is reasonable to consider these dimers as the relevant degree of freedom in the strongly coupled regime. The results presented above indicate that the two approaches yield consistent results, with or without inclusion of the repulsive intralayer interaction.

The crystalline phases [15–17] are also ground-state candidates due to the intralayer repulsion. For $W/d = 0.2$ used in our calculations, these phases could appear below the roton instability region in Fig. 1. The finite extent of the dimers is, however, still a concern, and further work is needed to determine the crystal phases in the bilayer setup.

In order to detect the phases a number of techniques could be applied. Dimerization in the layers should be detectable by Bragg scattering [47] or *in situ* nondemolition detection [48,49], whereas rf spectroscopy can probe the gap. To probe the finite-temperature physics, one can detect the associated vortices by matter-wave heterodyning [50]. To estimate parameters for relevant systems, we take $d = 0.5 \mu\text{m}$, which yields $U = 1.22$ for KRb molecules at $D = 0.566 D$ and $U = 4.15$ for LiCs at $D = 1.0 D$ (the permanent dipole moment of this molecule in the ground state is about $D = 5.4 D$ [51]). For densities $n = 10^5\text{--}10^8 \text{ cm}^{-2}$ we have $k_F d = 0.06\text{--}1.8$. The critical density to reach $\mu_{\text{BCS}} < 0$ is about $n \sim 0.2 \times 10^8 \text{ cm}^{-2}$, whereas the dimer BEC requires $n \lesssim 0.6 \times 10^7 \text{ cm}^{-2}$. Unfortunately, as $T_F = E_0(k_F d)^2/k_B$ this means that extremely low temperatures ($\lesssim 1 \text{ nK}$) are required to reach T_{BKT} .

Interesting directions for future work include investigation of more than two layers or tilting of the dipoles with respect to the plane. With dipoles that are no longer perpendicular, one can still show that a two-body bound dimer will be present for any value of the dipole moment [52], although the dimer binding energy is reduced [53]. In the single-layer case, *p*-wave superfluidity can occur for an extended range of tilting angles [11], and we expect similar effects for a bilayer. This setup can be explored with the same methods used here. In a setting with multiple layers, more phases should be expected, such as coherent density waves [36], pairing [47], and bound states with more than two molecules [35,54].

ACKNOWLEDGMENTS

We thank E. Demler, L. Pollet, A. S. Jensen, G. M. Bruun, and M. M. Parish for fruitful discussions and C.-H. Lin and I.-W. Tsai for early pioneering work. D.W.W. appreciates the hospitality of the JQI during the initial investigation of this project and acknowledges research and travel support from NCTS (Taiwan). Support by the Carlsberg Foundation and by the German Science Foundation under Grant No. WU 609/1-1 is gratefully acknowledged.

-
- [1] S. Ospelkaus *et al.*, *Nat. Phys.* **4**, 622 (2008).
 [2] K. K. Ni *et al.*, *Science* **322**, 231 (2008).
 [3] J. Deiglmayr, A. Grochola, M. Repp, K. Mortlbauer, C. Gluck, J. Lange, O. Dulieu, R. Wester, and M. Weidemuller, *Phys. Rev. Lett.* **101**, 133004 (2008).
 [4] F. Lang, K. Winkler, C. Strauss, R. Grimm, and J. H. Hecker Denschlag, *Phys. Rev. Lett.* **101**, 133005 (2008).
 [5] K. K. Ni *et al.*, *Nature (London)* **464**, 1324 (2010).
 [6] S. Ospelkaus *et al.*, *Science* **327**, 853 (2010).
 [7] M. A. Baranov, *Phys. Rep.* **464**, 71 (2008).
 [8] T. Lahaye, C. Menotti, L. Santos, M. Lewenstein, and T. Pfau, *Rep. Prog. Phys.* **72**, 126401 (2009).
 [9] D.-W. Wang, M. D. Lukin, and E. Demler, *Phys. Rev. Lett.* **97**, 180413 (2006).
 [10] D.-W. Wang, *Phys. Rev. Lett.* **98**, 060403 (2007).
 [11] G. M. Bruun and E. Taylor, *Phys. Rev. Lett.* **101**, 245301 (2008).
 [12] N. R. Cooper and G. V. Shlyapnikov, *Phys. Rev. Lett.* **103**, 155302 (2009).
 [13] R. M. Lutchyn, E. Rossi, and S. Das Sarma, *Phys. Rev. A* **82**, 061604(R) (2010).
 [14] M. Klawunn, J. Duhme, and L. Santos, *Phys. Rev. A* **81**, 013604 (2010).
 [15] C. Mora, O. Parcollet, and X. Waintal, *Phys. Rev. B* **76**, 064511 (2007).
 [16] H.-P. Büchler, E. Demler, M. Lukin, A. Micheli, N. Prokofev, G. Pupillo, and P. Zoller, *Phys. Rev. Lett.* **98**, 060404 (2007).
 [17] G. E. Astrakharchik, J. Boronat, I. L. Kurbakov, and Yu. E. Lozovik, *Phys. Rev. Lett.* **98**, 060405 (2007).
 [18] M. G. H. de Miranda *et al.*, *Nat. Phys.* **7**, 502 (2011).
 [19] S.-M. Shih and D.-W. Wang, *Phys. Rev. A* **79**, 065603 (2009).
 [20] J. R. Armstrong, N. T. Zinner, D. V. Fedorov, and A. S. Jensen, *Europhys. Lett.* **91**, 16001 (2010).
 [21] M. Klawunn, A. Pikovski, and L. Santos, *Phys. Rev. A* **82**, 044701 (2010).
 [22] W. Ketterle and M. W. Zwierlein, in *Ultracold Fermi Gases, in Proceedings of the International School of Physics “Enrico Fermi,” Course CLXIV, Varenna, 2006*, edited by M. Inguscio, W. Ketterle, and C. Salomon (IOS Press, Amsterdam, 2008).
 [23] V. L. Berezinskii, *Sov. Phys. JETP* **34**, 610 (1972).
 [24] J. M. Kosterlitz and D. J. Thouless, *J. Phys. C* **6**, 1181 (1973).
 [25] A. Pikovski, M. Klawunn, G. V. Shlyapnikov, and L. Santos, *Phys. Rev. Lett.* **105**, 215302 (2010).
 [26] M. A. Baranov, A. Micheli, S. Ronen, and P. Zoller, *Phys. Rev. A* **83**, 043602 (2011).
 [27] C. Zhao, L. Jiang, X. Liu, W. M. Liu, X. Zou, and H. Pu, *Phys. Rev. A* **81**, 063642 (2010).
 [28] Z. Li and K. Yamada, *J. Phys. Soc. Jpn.* **70**, 797 (2001).
 [29] M. Randeria, J.-M. Duan, and L.-Y. Shieh, *Phys. Rev. B* **41**, 327 (1990).
 [30] G. Bertainia and S. Giorgini, *Phys. Rev. Lett.* **106**, 110403 (2011).
 [31] N. T. Zinner, J. R. Armstrong, A. G. Volosniev, D. V. Fedorov, and A. S. Jensen, e-print arXiv:1105.6264.
 [32] L. Santos, G. V. Shlyapnikov, and M. Lewenstein, *Phys. Rev. Lett.* **90**, 250403 (2003).
 [33] U. R. Fischer, *Phys. Rev. A* **73**, 031602(R) (2006).
 [34] I. V. Brodsky, M. Yu. Kagan, A. V. Klaptsov, R. Combescot, and X. Leyronas, *Phys. Rev. A* **73**, 032724 (2006).
 [35] A. G. Volosniev, D. V. Fedorov, A. S. Jensen, and N. T. Zinner, e-print arXiv:1109.4602.
 [36] N. T. Zinner and G. M. Bruun, *Eur. Phys. J. D* **65**, 133 (2011).
 [37] M. Babadi and E. Demler, *Phys. Rev. B* **84**, 235124 (2011).
 [38] L. M. Sieberer and M. A. Baranov, *Phys. Rev. A* **84**, 063633 (2011).
 [39] M. M. Parish and F. M. Marchetti, e-print arXiv:1109.2464.

- [40] J. K. Block, N. T. Zinner, and G. M. Bruun (unpublished).
- [41] C.-H. Lin, Y.-T. Hsu, H. Lee, and D.-W. Wang, *Phys. Rev. A* **81**, 031601(R) (2010).
- [42] K. Sun, C. Wu, and S. DasSarma, *Phys. Rev. B* **82**, 075105 (2010).
- [43] Y. Yamaguchi, T. Sogo, T. Ito, and T. Miyakawa, *Phys. Rev. A* **82**, 013643 (2010).
- [44] K. Miyake, *Prog. Theor. Phys.* **69**, 1794 (1983).
- [45] U. C. Tauber and D. R. Nelson, *Phys. Rep.* **289**, 157 (1997).
- [46] A. Filinov, N. V. Prokof'ev, and M. Bonitz, *Phys. Rev. Lett.* **105**, 070401 (2010).
- [47] A. C. Potter, E. Berg, D.-W. Wang, B. I. Halperin, and E. Demler, *Phys. Rev. Lett.* **105**, 220406 (2010).
- [48] B. Wunsch, N. T. Zinner, I. B. Mekhov, S.-J. Huang, D.-W. Wang, and E. Demler, *Phys. Rev. Lett.* **107**, 073201 (2011).
- [49] N. T. Zinner, B. Wunsch, I. B. Mekhov, S. J. Huang, D.-W. Wang, and E. Demler, *Phys. Rev. A* **84**, 063606 (2011).
- [50] P. Krüger *et al.*, *Nature (London)* **441**, 1118 (2006).
- [51] J. Deiglmayr, A. Grochola, M. Repp, O. Dulieu, R. Wester, and M. Weidemüller, *Phys. Rev. A* **82**, 032503 (2010).
- [52] A. G. Volosniev, D. V. Fedorov, A. S. Jensen, and N. T. Zinner, *Phys. Rev. Lett.* **106**, 250401 (2011).
- [53] A. G. Volosniev, N. T. Zinner, D. V. Fedorov, A. S. Jensen, and B. Wunsch, *J. Phys. B* **44**, 125301 (2011).
- [54] J. R. Armstrong, N. T. Zinner, D. V. Fedorov, and A. S. Jensen, e-print arXiv:1106.2102.